Ferroelectrics

Ab Initio Calculations of the Atomic and Electronic Structure of SrZrO$_3$ (111) Surfaces

R. I. Eglitis [a]

[a] Institute of Solid State Physics, University of Latvia, 8 Kengaraga Str., Riga, LV1063, Latvia

PLEASE SCROLL DOWN FOR ARTICLE

Ab Initio Calculations of the Atomic and Electronic Structure of SrZrO₃ (111) Surfaces

R. I. EGLITIS*

Institute of Solid State Physics, University of Latvia, 8 Kengaraga Str.,
Riga LV1063, Latvia

The paper presents and discusses the results of calculations of surface relaxations and energetics for the polar (111) surface of SrZrO₃ using a hybrid B3LYP description of exchange and correlation. On the (111) surface, I consider both Zr- and SrO₃-terminations. For both Zr and SrO₃-terminated SrZrO₃ (111) surfaces upper layer atoms relax inwards. The second layer atoms, with the sole exception of Zr-terminated SrZrO₃ (111) surface Sr atom, relax outwards. The calculated surface relaxation energy for Zr-terminated SrZrO₃ (111) surface is almost sixteen times larger, than the surface relaxation energy for SrO₃-terminated SrZrO₃ (111) surface. The surface energy for Zr-terminated SrZrO₃ (111) surface (7.98 eV) is smaller, than the surface energy for SrO₃-terminated SrZrO₃ (111) surface (9.45 eV).

Keywords *Ab initio* calculations; (111) surfaces; SrZrO₃; B3LYP

Introduction

Thin films of ABO_3 perovskite ferroelectrics play an important role in numerous microelectronic, catalytic, and other high-technology applications, and are frequently used as substrates for growth of other materials such as cuprate superconductors [1,2]. Therefore, it is not surprising that a large number of *ab initio* quantum-mechanical calculations have dealt with the atomic and electronic structures of the (001) and (011) surfaces of $SrTiO_3$, $BaTiO_3$, $PbTiO_3$, $CaTiO_3$, $BaZrO_3$ and $SrZrO_3$ crystals [3–13].

Due to intensive development and progressive miniaturization of electronic devices, the surface structure as well as the electronic properties of the ABO_3 perovskite thin films have been extensively studied experimentally in recent years. For example, the $SrTiO_3$ (001) surface structure has been analyzed by means of low-energy electron diffraction (LEED) [14], reflection high-energy electron diffraction (RHEED) [15], x-ray photoelectron spectroscopy (XPS), ultraviolet electron spectroscopy, medium-energy ion scattering [16], and surface x-ray diffraction [17]. The most recent experimental studies on the $SrTiO_3$ surfaces include a combination of XPS, LEED, and time-of-flight scattering and recoil spectrometry (TOF-SARS) [18], as well as metastable impact electron spectroscopy [19].

As it is well known, the $SrZrO_3$ compound shows a cubic perovskite-type crystal structure. The space group (P_{m3m}: 221) contains 48 symmetry operations including inversion. The Wyckoff positions of the atoms are Sr 1a (0.0, 0.0, 0.0), Zr 1b (0.5, 0.5, 0.5) and O 3c

---

(0.0, 0.5, 0.5). The $SrZrO_3$ crystal undergoes at least three phase transitions as follows. Orthorhombic (P_{nma}) orthorhombic (C_{mcm}) tetragonal ($I4/_{mcm}$) cubic (P_{m3m}) at 970 K, 1100 K, and 1440 K, respectively. $SrZrO_3$ has a rather high melting temperature of about 2647°C and thereby it is cubic in a wide range of temperature where most of its applications take place. Therefore, in this work, I performed $SrZrO_3$ (111) polar surface calculations for its high symmetry cubic phase.

Taking into account this high technological importance, it is surprising that there have been no *ab initio* studies dealing with $SrZrO_3$ (111) polar surface. In this study first predictive *ab initio* calculations dealing with atomic and electronic structure of $SrZrO_3$ (111) surface structures are performed. The manuscript is organized as follows. In Sec. II computational details are presented. The results of calculations for surface structures, energies, charge distributions, and band populations are reported in Sec. III. Finally, the results are discussed and conclusions are presented in Sec. IV.

Computational Details

To perform the first-principles DFT-B3LYP calculations, I used the CRYSTAL computer code [20]. This code employs Gaussian-type functions (GTF) localized at atoms as the basis for an expansion of the crystalline orbitals. Features of the CRYSTAL code, which are most important for the study of perovskite surfaces, present its ability to calculate the electronic structure of materials within both HF and Kohn-Sham (KS) Hamiltonians and implementation of the isolated 2D slab model without its artificial repetition along the *z*-axis. However, in order to employ the linear combination of atomic orbitals (LCAO)-GTF method, it is desirable to have optimized basis sets (BS). The optimization of such BSs for $SrTiO_3$, $BaTiO_3$ and $PbTiO_3$ perovskites was developed and discussed by Piskunov *et al*. [21]. In the present paper, for O atoms, we have used this new BS which differs from the previous calculations [22,23] by inclusion of polarisable *d*-orbitals on O ions. For Sr and Zr atoms I used the same basis set as in Refs. [12,13].

My calculations have been performed using the hybrid exchange-correlation B3LYP functional involving a hybrid of nonlocal Fock exact exchange, LDA exchange and Beckes gradient corrected exchange functional [24], combined with the nonlocal gradient corrected correlation potential by Lee-Yang-Parr [25]. The Hay-Wadt small-core effective core pseudopotentials (ECP) have been adopted for Sr and Zr atoms [26,27]. The small-core ECPs replace only inner core orbitals, but orbitals for sub-valence electrons as well as for valence electrons are calculated self-consistently. Light oxygen atoms have been treated with the all-electron BS [21].

The reciprocal space integration has been performed by sampling the Brillouin zone of the five-atom cubic unit cell with the $5 \times 5 \times 1$ Pack-Monhorst net [28], that provides the balanced summation in direct and reciprocal spaces. To achieve high accuracy, large enough tolerances of 7, 8, 7, 7, 14 have been chosen for the Coulomb overlap, Coulomb penetration, exchange overlap, the first exchange pseudo-overlap, and for the second exchange pseudo-overlap, respectively [20].

The $SrZrO_3$ (111) surfaces have been modeled with two-dimensional (2D) slabs, consisting of several planes perpendicular to the [111] crystal direction. The CRYSTAL code has allowed to avoid artificial periodicity along the Oz direction and to perform calculations for stand-alone 2D slabs. To simulate $SrZrO_3$ (111) surfaces, I have implemented symmetrical (with respect to the mirror plane) slabs consisting of nine alternating Zr and
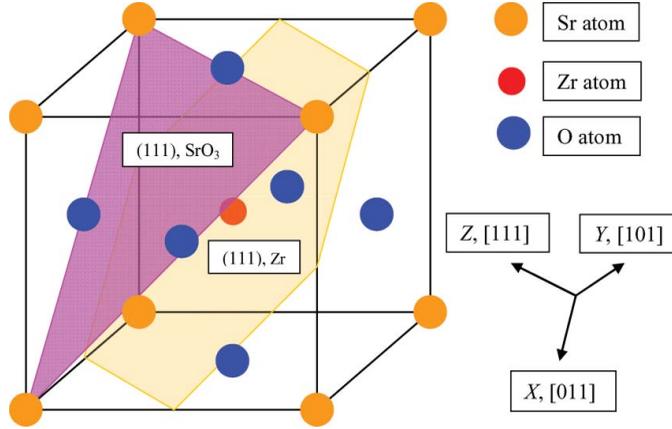
Figure 1. Two possible terminations of the polar $SrZrO_3$ (111) surface: SrO_3 and Zr.

SrO_3 layers. One of these slabs is terminated by Zr planes and consists of a supercell containing 21 atoms. The second slab is terminated by SrO_3 planes and consists of a supercell containing 24 atoms. These slabs are non-stoichiometric, with unit cell formulas $Sr_4Zr_5O_{12}$ and $Sr_5Zr_4O_{15}$, respectively. These two (Zr and SrO_3) terminations are the only two possible flat and dense (111) surfaces in $SrZrO_3$ perovskite lattice structure. I created the Zr- and SrO_3-terminated (111) slabs from the high symmetry cubic $SrZrO_3$ structure with the space group (P_{m3m}: 221) (see Fig. 1). I performed the geometry relaxation of Zr- and SrO_3-terminated $SrZrO_3$ (111) slabs only along the symmetry allowed z axis.

As the next step, I have calculated cleavage and surface energies. It is obvious that Zr and SrO_3-terminated (111) surfaces are mutually complementary. The cleavage energy of the complementary surface $E_{cl}(\lambda)$ ($\lambda = Zr$ or SrO_3) can be obtained from the total energies computed for the unrelaxed slabs through the following equation:

$$E_{cl}(\lambda) = \frac{1}{4}\big[E_{slab}^{unrel}(Zr) + E_{slab}^{unrel}(SrO_3) - 9E_{bulk}\big] \tag{1}$$

where $E_{slab}^{unrel}(\lambda)$ is the total energy of unrelaxed λ-terminated slab, E_{bulk} is the bulk energy per formula unit in the cubic structure, and $1/4$ means that totally four surfaces are created upon the crystal cleavage.

When both sides of the slab are allowed to relax, the relaxation energies for each of the surfaces can be obtained by the equation:

$$E_{rel}(\lambda) = \frac{1}{2}\big[E_{slab}^{rel}(\lambda) - E_{slab}^{unrel}(\lambda)\big] \tag{2}$$

where $E_{slab}^{rel}(\lambda)$ is the λ-terminated slab energy after relaxation, $1/2$ means that two surfaces are created upon the crystal cleavage. Now when the cleavage and relaxation energies are calculated, the surface energy is just a sum of them:

$$E_{surf}(\lambda) = E_{cl}(\lambda) + E_{rel}(\lambda) \tag{3}$$

Table 1

Calculated effective charges Q and bond populations P (in e) for bulk $SrZrO_3$

Ion or bond	Property	Value
	$SrZrO_3$	
Sr	Q	$+1.880$
O	Q	-1.351
Zr	Q	$+2.174$
Sr-O	P	$+0.002$
Zr-O	P	$+0.092$
O-O	P	-0.008

Main Results

As a starting point of the calculations, the $SrZrO_3$ bulk lattice constant has been calculated. The calculated bulk lattice constant for $SrZrO_3$ (4.195 Å) is slightly larger than the experimental value of 4.109 Å [29]. Thus, the computational approach used in the present study can be established as appropriate. I used the theoretical $SrZrO_3$ bulk lattice constant in the following $SrZrO_3$ polar (111) surface structure calculations.

    To characterize the chemical bonding and covalency effects, I have applied a standard Mulliken population analysis for the effective atomic charges Q and other local properties of electronic structure as described, for example, in [30]. My calculated effective charges for the $SrZrO_3$ bulk are ($+1.880e$) for the Sr atom, ($+2.174e$) for the Zr atom, and ($-1.351e$) for the O atom (see Table 1). The bond population of the chemical bonding between Zr and O atoms is ($+0.092e$) in $SrZrO_3$. The bond populations between Sr and O atoms in SrZrO3 ($+0.002e$) are much smaller. Finally, the bond populations between O and O atoms in $SrZrO_3$ ($-0.008e$) are negative, which indicates repulsion between O-O atoms (see Table 1).

Table 2

Calculated relaxation of Zr- and SrO_3-terminated $SrZrO_3$ (111) surface upper three layer atoms (as a percentage of the bulk crystal lattice constant $a_o = 4.195$ Å). Positive (negative) values refer to displacements in the direction outwards (inwards) the surface

Layer	Ion	Displacement (Dz)
	Zr-terminated $SrZrO_3$ (111) surface	
1	Zr	-5.72
2	Sr	-11.92
	O	$+0.79$
3	Zr	$+1.53$
	SrO_3-terminated $SrZrO_3$ (111) surface	
1	Sr	-0.74
	O	-0.52
2	Zr	$+0.74$
3	Sr	-0.02
	O	-0.18

Table 3

Calculated cleavage, relaxation, and surface energies for $SrZrO_3$ (111) surfaces (in electron volt per surface cell)

Surface	Termination	$E_{(cl)}$	$E_{(rel)}$	$E_{(surf)}$
$SrZrO_3$ (111)	Zr-term.	9.55	−1.57	7.98
	SrO_3-term.	9.55	−0.10	9.45

According to the results of my calculations, the upper layer Zr atom for Zr-terminated $SrZrO_3$ (111) surface strongly (by 5.72% of bulk lattice constant a_o) relaxes inwards towards the bulk (see Table 2). The second layer Sr atom relaxes inwards even more strongly (by 11.92% of a_o), while the second layer O atom relaxes outwards by 0.79% of a_o. Outward relaxation of the third layer Zr atom is rather weak, only 1.53% of a_o.

For SrO_3-terminated $SrZrO_3$ (111) surface the upper layer metal and oxygen atoms relaxes inwards by 0.74% of a_o and 0.52% of a_o, respectively (see Table 2). The second layer Zr atom outward relaxation magnitude (0.74% of a_o) is exactly the same as the upper layer Sr atom inward relaxation. Both third layer Sr and O atoms relax inwards by a very small magnitude (0.02% of a_o and 0.18% of a_o), respectively.

The calculated surface relaxation energy for Zr-terminated $SrZrO_3$ (111) surface (−1.57 eV) is almost sixteen times larger, than the surface relaxation energy for SrO_3-terminated $SrZrO_3$ (111) surface (−0.10 eV) (see Table 3). The calculated surface energy for Zr-terminated $SrZrO_3$ (111) surface is equal to 7.98 eV, while the surface energy for SrO_3-terminated $SrZrO_3$ (111) surface is equal to 9.45 eV.

Conclusions

By means of the hybrid B3LYP approach, the Zr- and SrO_3-terminated $SrZrO_3$ polar (111) surface relaxations has been calculated. For both Zr- and SrO_3-terminated $SrZrO_3$ (111) surfaces the upper layer atoms relax inwards. The second layer atoms, with the sole exception of Zr-terminated $SrZrO_3$ (111) surface Sr atom, relax outwards. Both third layer Sr and O atoms on the SrO_3-terminated $SrZrO_3$ (111) surface relax inwards, while the third layer Zr atom on the Zr-terminated $SrZrO_3$ (111) surface relax outwards. The Zr-terminated $SrZrO_3$ (111) surface second layer Sr atom exibits the strongest relaxation between all Zr and SrO_3-terminated $SrZrO_3$ (111) surface atoms.

The calculated surface relaxation energy for Zr-terminated $SrZrO_3$ (111) surface is almost sixteen times larger than the surface relaxation energy for SrO_3-terminated $SrZrO_3$ (111) surface. The surface energy for Zr-terminated $SrZrO_3$ (111) surface (7.98 eV) is smaller, than the surface energy for SrO_3-terminated (111) surface (9.45 eV).

Acknowledgments

References

1. J. F. Scott, *Ferroelectric Memories*. Springer: Berlin; 2000.
2. M. E. Lines and A. M. Glass, *Principles and Applications of Ferroelectrics and Related Materials*. Clarendon: Oxford; 1977.

3. N. Erdman, K. R. Poeppelmeier, M. Asta, O. Warschkow, D. E. Ellis, and L. D. Marks, The structure and chemistry of the TiO_2-rich surface of $SrTiO_3$ (001). *Nature* **419**, 55–57 (2002).

4. R. I. Eglitis and D. Vanderbilt, First-principles calculations of atomic and electronic structure of $SrTiO_3$ (001) and (011) surfaces. *Phys. Rev.* **B 77**, 195408 (2007).

5. E. A. Kotomin, R. I. Eglitis, J. Maier, and E. Heifets, Calculations of the atomic and electronic structure for $SrTiO_3$ perovskite thin films. *Thin Solid Films* **400**, 76–80 (2001).

6. A. Hofer, M. Fechner, K. Duncker, M. Holzer, I. Mertig, W. Widdra, Persistence of surface domain structures for a bulk ferroelectric above T-C. *Phys. Rev. Lett.* **108**, 087602 (2012).

7. R. I. Eglitis, G. Borstel, E. Heifets, S. Piskunov, and E. Kotomin, *Ab initio* calculations of the $BaTiO_3$ (100) and (110) surfaces. *Journal of Electroceramics.* **16**, 289–292 (2006).

8. M. Stengel, Electrostatic stability of insulating surfaces: Theory and applications. *Phys. Rev. B* **84**, 205432 (2011).

9. R. I. Eglitis and D. Vanderbilt, *Ab initio* calculations of the atomic and electronic structure of $CaTiO_3$ (001) and (011) surfaces. *Phys. Rev. B* **78**, 155420 (2008).

10. A. M. Kolpak, D. Li, R. Shao, A. M. Rappe, and D. A. Bonnell, *Phys. Rev. Lett.* **101**, 036102 (2008).

11. R. I. Eglitis and D. Vanderbilt, *Ab initio* calculations of $BaTiO_3$ and $PbTiO_3$ (001) and (011) surface structures. *Phys. Rev. B* **76**, 155439 (2007).

12. R. I. Eglitis, First-principles calculations of $BaZrO_3$ (001) and (011) surfaces. *J. Phys.: Condens. Matter* **19**, 356004 (2007).

13. R. I. Eglitis and M. Rohlfing, First-principles calculations of the atomic and electronic structure of $SrZrO_3$ and $PbZrO_3$ (001) and (011) surfaces. *J. Phys.: Condens. Matter* **22**, 415901 (2010).

14. N. Bickel, G. Schmidt, K. Heinz, and K. Müller, Ferroelectric relaxation of the $SrTiO_3$ (100) surface. *Phys. Rev. Lett.* **62**, 2009–2011 (1989).

15. T. Hikita, T. Hanada, M. Kudo, and M. Kawai, Structure and electronic state of the TiO_2 and SrO terminated $SrTiO_3$ (100) surfaces. *Surf. Sci.* **287–288**,377–381 (1993).

16. A. Ikeda, T. Nishimura, T. Morishita, and Y. Kido, *Surf. Sci.* **433–435**, 520–524 (1999).

17. G. Charlton, S. Brennan, C. A. Muryn, R. McGrath, D. Norman, T. S. Turner, and G. Thorthon, Surface relaxation of $SrTiO_3$ (001). *Surf. Sci.* **457**, L376–L380 (2000).

18. P. A. W. Heide, Q. D. Jiang, Y. S. Kim, and J. W. Rabalais, X-ray photoelectron spectroscopic and ion scattering study of the $SrTiO_3$ (001) surface. *Surf. Sci.* **473**, 59–70 (2001).

19. W. Maus-Friedrichs, M. Frerichs, A. Gunhold, S. Krischok, V. Kempter, and G. Bihlmayer, The characterization of $SrTiO_3$ (001) with MIES, UPS(Hel) and first-principles calculations. *Surf. Sci.* **515**, 499–506 (2002).

20. V. R. Saunders, R. Dovesi, C. Roetti, M. Causa, N. M. Harrison, R. Orlando, and C. M. Zicovich-Wilson, *CRYSTAL-2006 User Manual. University of Torino*. Torino, Italy; 2006.

21. S. Piskunov, E. Heifets, R. I. Eglitis, and G. Borstel, Bulk properties of $SrTiO_3$, $BaTiO_3$ and $PbTiO_3$ perovskites: an *ab initio* HF/DFT study. *Comput. Mater. Sci.* **29**, 165–180 (2004).

22. E. Heifets, R. I. Eglitis, E. A. Kotomin, J. Maier, and G. Borstel, *Ab initio* modeling of surface structure for $SrTiO_3$ perovskite crystals. *Phys. Rev. B.* **64**, 235417 (2001).

23. E. Heifets, R. I. Eglitis, E. A. Kotomin, J. Maier, and G. Borstel, First-principles calculations for $SrTiO_3$ (100) surface structure. *Surf. Sci.* **513**, 211–220 (2002).

24. A. B. Becke, Density-functional thermochemistry. III. The role of exact exchange. *J. Chem. Phys.* **98**, 5648–5652 (1993).

25. C. Lee, W. Yang, and R. G. Parr, Development of the Colle-Salvetti correlation-energy formula into a functional of the electron density. *Phys. Rev. B* **37**, 785–789 (1988).

26. P. J. Hay and W. R. Wadt, *Ab initio* effective core potentials for molecular calculations. Potentials for K to Au including the outermost core orbitals. *J. Chem. Phys.* **82**, 299–310 (1985).

27. W. R. Wadt and P. J. Hay, *Ab initio* effective core potentials for molecular calculations. Potentials for main group element Na to Bi. *J. Chem. Phys.* **82**, 284–298 (1985).

28. H. J. Monkhorst and J. D. Pack, Special points for Brillouin-zone integrations. *Phys. Rev. B* **13**, 5188–5192 (1976).
29. A. J. Smith and A. J. Welch, Some mixed metal oxides of perovskite structure. *Acta Crys.* **13**, 653–656 (1960).
30. C. R. A. Catlow and A. M. Stoneham, Ionicity in solids. *J. Phys. C: Solid State Phys.* **16**, 4321–4338 (1983).